

# Evidence for room temperature superconductivity at graphite interfaces

Pablo D. Esquinazi, Christian E. Precker, Markus Stiller, Tiago R. S.

Cordeiro, José Barzola-Quiquia, Annette Setzer, and Winfried Böhlmann

*Division of Superconductivity and Magnetism, Felix Bloch Institute for Solid State Physics,  
Universität Leipzig, Linnéstraße 5, D-04103 Leipzig, Germany*

In the last 43 years several hints were reported suggesting the existence of granular superconductivity above room temperature in different graphite-based systems. In this paper some of the results are reviewed, giving special attention to those obtained in water and n-heptane treated graphite powders, commercial and natural bulk graphite samples with different characteristics as well as transmission electron microscope (TEM) lamellae. The overall results indicate that superconducting regions exist and are localized at certain internal interfaces of the graphite structure. The existence of the rhombohedral graphite phase in all samples with superconducting-like properties suggests its interfaces with the Bernal phase as a possible origin for the high-temperature superconductivity, as theoretical calculations predict. High precision electrical resistance and magnetization measurements were used to identify a transition at  $T_c \gtrsim 350$  K. To check for the existence of true zero resistance paths in the samples we used local magnetic measurements, which results support the existence of superconducting regions at such high temperatures.

## I. FIRST HINTS FOR ROOM TEMPERATURE SUPERCONDUCTIVITY IN DISORDERED GRAPHITE POWDERS

In the year 1974 Kazimierz Antonowicz published studies [1] on current-voltage  $I - V$  characteristics curves of annealed carbon powder contacted between two Al electrodes. He recognized a kind of “critical current”  $I_c$  from the  $I - V$  curves and measured the influence of low amplitude applied magnetic fields on  $I_c$ . The result is reproduced in Fig. 1(a). The field dependence of this “critical current”  $I_c$  follows the field dependence given by the Josephson critical current equation  $I_c = |I_0 \sin(x)/x + I_1|$  whereas  $x \propto H$ ,  $H$  the applied field and  $I_1$  a field-independent constant background current. This constant as well as the field  $\Delta H$  at which  $I_c$  shows the first minimum are sample dependent, the last between 0.1 Oe  $< \Delta H < 1$  Oe [1].

The observed behavior in Fig. 1(a) follows the maximum net supercurrent equation for a Josephson junction under a magnetic field in the plane of the junction, referred to as Fraunhofer diffraction pattern, see e.g. [3]. There are several details we should note before arguing against or for a possible interpretation on the basis of a Josephson superconducting junction. Namely, the way the sample and the contacts were prepared did not allow for a direct contact to the possible superconducting junctions, which may explain the finite background  $I_1$ . If we assume that the observed behavior is indeed due to a Josephson junction the field variable  $x = \pi\Phi/\Phi_0$ , where the enclosed magnetic flux for a rectangular junction of thickness  $d$  and length  $L$  (normal to the applied field), see Fig. 1(c), would be  $\Phi = (2\lambda + d)LH\mu_0$  with  $\lambda$  the London penetration depth. The range of field  $\Delta H$  where the first minimum was observed would indicate a rather large area  $\sim 10 \mu\text{m}^2 < (2\lambda + d)L < \sim 100 \mu\text{m}^2$ . Assuming that there are superconducting regions coupled through a non-superconducting path in the annealed graphite powder, how could be possible that Cooper pairs tunnel through

a rather large carbon matrix? On the other hand, if instead of a three dimensional a two dimensional (2D) junction is formed, as we may have at certain interfaces (see Section III), taking into account that Cooper pairs can survive large distances in a graphene layer [4] and the expected enhancement of the effective London penetration depth in this 2D case [5], such a behavior does not appear impossible.

The same author published one year later the behavior of the  $I - V$  curves of the same annealed carbon powder at room temperature but irradiated with radiation of 10 GHz frequency [2], see Fig. 1(b). For an ideal Josephson junction we would expect that this radiation produces constant-voltage Shapiro steps [6] in the DC  $I - V$  curves at voltages  $V_n = n\hbar\omega/2e$ , with  $n$  an integer and  $\omega$  the angular frequency of radiation. For  $\omega = 2\pi 10^{10}$  Hz we expect certain steps in the  $I - V$  curves at voltages  $V_n = n20 \mu\text{V}$ , several orders of magnitude smaller than the observed 120 mV, see Fig. 1(b). Following the author explanation for this large voltage difference, one notes that the used experimental setup did not test only the voltage coming from the apparent Josephson junction but also the one provided by extra resistances, see inset in Fig. 1(b). The value of those resistance remained, however, unknown.

Independently of the uncertainties in the interpretation of the experimental results shown in Fig. 1, perhaps the main obstacle we have to believe on the results reported in [1, 2] is the fact that they were obtained at room temperature. If we assume that the experiment and its interpretation are correct, there are further details written explicitly in those publications [1, 2] that one should take into account if one wants to repeat the experiments, namely: The “new superconducting state” is quasi-stable, detectable for a few hours or it vanishes within a few days, and, only  $\sim 30\%$  of the “properly produced” samples showed the effect. These hints would indicate a superconductor very sensitive to the preparation details and rather unstable. It is appealing to argue

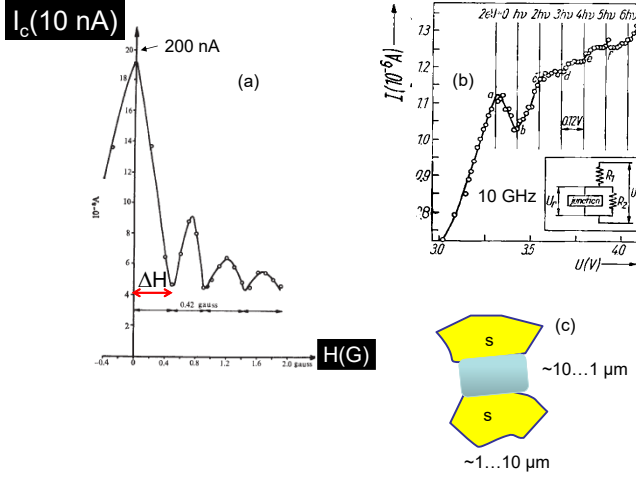


FIG. 1. (a) Maximum critical current vs. applied magnetic field deduced from current-voltages curves obtained from annealed carbon powder under an input current through two Al electrodes at room temperature. Upon sample, the field value at the first minimum is  $\Delta H = 0.1 \dots 1$  G. Adapted from [1]. (b) Current-voltage characteristic line obtained at room temperature for a similar annealed graphite powder as in (a) under a radiation of 10 GHz frequency. The inset shows the effective electric circuit proposed to explain the large voltage values between the apparent steps. The values of the resistance  $R_1, R_2$  are unknown. Adapted from [2]. (c) Sketch of a Josephson junction with the superconducting parts (yellow boxes) and the (blue) region representing the tunnel barrier plus the area where the magnetic flux produced by an applied magnetic field applied normal to the area enters. This (blue) area would be given by  $(2\lambda + d)L$ , which would be  $\sim 10 \dots 100 \mu\text{m}^2$ , according to the range of fields where the first minimum was measured [1], see (a).

that the origin of the measured signals should be related to certain interfaces between graphite-like grains.

All these details clearly prevented a quick reproduction of the published results added to the huge skepticism of the scientific community. We are not aware of any published report showing similar results as those in [1, 2]. In what follows we review some magnetization results obtained in water and n-heptane treated high-quality graphite powders that suggest that granular superconductivity might be indeed possible in the powders, very probably at certain interfaces created after the corresponding treatments [7, 8].

## II. MAGNETIZATION MEASUREMENTS ON GRAPHITE POWDERS

In this section we discuss results obtained from graphite powders that support to some extent the results discussed in Section I. The magnetization results of graphite powders, after a certain water or alkane

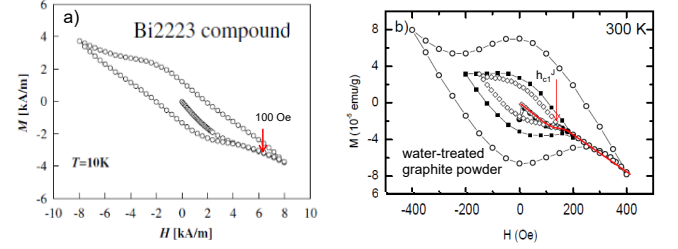


FIG. 2. a) Field dependence of the magnetization of a Bi2223 high- $T_c$  oxide granular compound at 10 K, adapted from [9]. b) Similar plot for a water-treated graphite powder at different maximum applied fields at 300 K, after subtraction of linear in field diamagnetic background, adapted from [7].

treatment, indicate a granular superconducting behavior that support the existence of superconducting regions in graphite and, indirectly, the possibility to have Josephson junctions in some regions.

The behavior of the magnetization of granular superconductors has been very well described in several works in the last 25 years, see e.g. [9, 10]. Due to the granularity and the Josephson coupling between grains, the strength of an applied magnetic field influences in a non simple way the field hysteresis. For example, at fields lower than the first critical field of the grains  $H_{c1}$  and lower than the field  $h_{c1}^J$  necessary to destroy the weakest links between the grains, a granular sample shows a Meissner-like response. At fields above  $h_{c1}^J$  but below the field  $h_{c2}^J$  (where the coupling between grains is completely overwhelmed and the magnetization is imposed by the London currents circulating around each of the grains) the hysteresis loop has a peculiar shape as shown in Fig. 2(a) [10]. At fields above  $h_{c2}^J$  but below the intrinsic  $H_{c1}$  of the grains, the hysteresis vanishes up to the field  $H_{c1}$ , at which Abrikosov vortices enters in the grains and field hysteresis loops are again measured due to their finite pinning in the superconducting matrix [10].

The magnetization of an untreated, very pure graphite powder, does not show any remarkable hysteresis [7]. However, after a treatment with water [7] or n-heptane (following the work in [11]) a clear irreversibility in field and in temperature is observed. As example, Fig. 2(b) shows the hysteresis loops of water-treated graphite powder at 300 K and at different maximum applied fields, after subtraction of a linear diamagnetic background. The hysteresis loops at fields below and above  $h_{c1}^J$  are qualitatively similar to the one obtained in granular superconductors, see Figure 2(a) and also [9, 10]. Similar curves were obtained after treatment the graphite powder with alkanes. The field hysteresis loops, the hysteresis in temperature, i.e. difference between the magnetization at field cooled (FC) and zero field cooled (ZFC) [7], suggest the existence of granular superconductivity at certain regions formed after the liquid treatment. Because a similar behavior is observed in graphite samples with

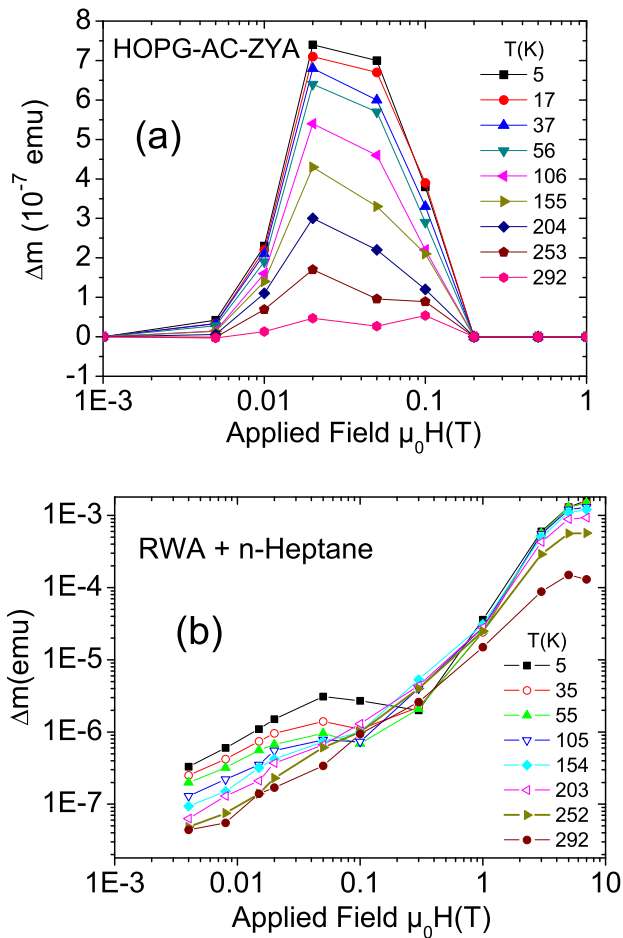


FIG. 3. The difference between FC and ZFC curves  $\Delta m$  as a function of applied field at different temperatures for the: (a) bulk HOPG sample (field applied parallel to the graphene planes), which magnetization shows a ferromagnetic hysteresis loop and (b) a n-heptane-treated graphite powder, which shows a field hysteresis similar to that of water treated graphite powder, see Fig. 2(b) and [7].

interfaces [8], it is appealing to suggest that certain interfaces are produced after the liquid treatment of the graphite grains. We note that the measurements were always done after the corresponding liquid was evaporated. An important experimental fact should be also stressed: If we apply pressure to the treated powder, the hysteresis loop vanishes, indicating that the hysteresis does not appear to be due to defect-induced magnetic order but it comes from certain regions of the graphite grains that are destroyed with pressure [7].

#### A. Thermomagnetic hysteresis measurements help to differentiate between a superconducting and ferromagnetic behavior

In some cases the measurement of the intrinsic field hysteresis of the superconducting regions is not straightforward to obtain because of, either, a much larger magnetic background coming from the rest of the sample, or because the size of the superconducting grains is too small and the effective pinning strength for the magnetic entities is too weak to be measured through a difference between ZFC and FC measurements. The superconducting-like signals obtained in graphite samples from magnetization measurements are mostly obtained after the necessary subtraction of a large diamagnetic background [12]. Although this background is intrinsically non-hysteretic, its contribution in real samples overwhelms the signals of interest by up to two orders of magnitude, see, e.g., [8, 12]. In this case one may doubt whether the subtraction of the diamagnetic slope is correctly done to obtain results like in, e.g., Fig. 2(b). In other words, if one subtracts a tiny different diamagnetic slope from the original data, in some cases one may transform the superconducting hysteresis loops in ferromagnetic-like loops. Therefore, one needs a background independent method that can rule out one of the two possible origins for the hysteresis.

The thermomagnetic hysteresis (TH), i.e., the difference between zero field cooling (ZFC) and field cooling (FC) curves at different constant applied magnetic fields, is an important experimental method to check for the existence of pinning or magnetic anisotropy of different kinds of magnetic entities, like, e.g., flux lines in superconductors as well as magnetic domains in magnetically ordered materials. Thermomagnetic hysteresis is specially useful to search for the existence of superconductivity in materials where only a very small fraction of this phase exists, like in granular superconductors.

In this work we studied the thermomagnetic response of different graphite samples, in particular of ultra pure graphite powders after n-heptane treatment. The study of the influence of n-heptane on graphite flakes follows the results reported in Ref. [11]. We note, however, that the obtained results are similar to graphite powders after water treatment. The main results of this work is that the thermomagnetic hysteresis helps to differentiate a ferromagnetic from a superconducting behavior, supporting the superconducting interpretation of the field hysteresis in [7, 8, 12].

The TH measurements of the magnetic moment  $\Delta m(T) = m_{FC}(T) - m_{ZFC}(T)$  obtained from different graphite powders and bulk samples were performed using a commercial MPMS-7 SQUID magnetometer. The temperature sweeps at fixed fields, applied always at 5 K (ZFC state), were done with rates between 1 and 5 K/min. The differences in the observed hysteresis between the rates lied within experimental error of  $\Delta m(T)/m(T) < 0.3\%$ . The used graphite powder was

the same as previously reported [7], i.e. RWA/T from SGL Carbon GmbH (Werk Ringsdorf, Germany) with very low impurity concentration (e.g.,  $\text{Fe} < 0.19 \mu\text{g/g}$ ). Further characterization of this graphite powder and the influence of water on its magnetization was thoroughly reported in [7]. In this study we found that if we follow the same procedure to treat the graphite powder with n-heptane as was done with water, i.e. continuously stirring of the graphite powder at room temperature for 24 h with 20 mL n-heptane (p.a. 99.99, Sigma-Aldrich) and then filtered and dried at 100 C overnight, the change in the magnetization was negligible. However, if the TH measurements of the graphite powder started immediately after dropping a droplet of n-heptane, the magnetization showed a behavior similar to the water-treated graphite. All the powders were packed in polymer foil (mass < 10 mg). The magnetization of this foil was measured independently and it gives a negligible magnetic moment in all the here reported measurements in comparison with the measured powder samples.

For comparison, we measured also: the untreated graphite powder (RWA-virgin), a pellet obtained from a high-purity graphite cylinder used for spectroscopy calibration (SK-AS01) and a graphite bulk sample (HOPG-AC-ZYA) from Advanced Ceramics, which impurity concentration and magnetization behavior was thoroughly characterized in [13]. This last bulk sample shows a ferromagnetic response for fields parallel to the graphene planes, originated by defects and/or hydrogen with a saturation field of  $\mu_0 H_{\text{sat}} \simeq 0.2 \text{ T}$  [13]. Similar field hysteresis curves at 300 K and the corresponding XMCD hysteresis on the carbon K-edge can be seen in [14].

In general the TH curve of a ferromagnetic sample as a function of applied magnetic field starts at zero at zero field and tends to vanish when the applied field is larger than the saturation field. The reason for the behavior at large enough fields is easy to understand. At the saturation field the sample is in one domain state and no difference is measured between  $m_{\text{FC}}(T)$  and  $m_{\text{ZFC}}(T)$ . The TH results for the graphite bulk sample with ferromagnetic behavior are presented in Fig. 3(a). We see that the TH shows a maximum at  $\sim 0.02 \text{ T}$  and vanishes at the saturation field of 0.2 T. The overall hysteresis increases the lower the temperature, as expected for magnetic graphite.

Similar TH measurements of the n-heptane treated graphite powder with superconducting like field hysteresis (as in [7, 8]) show a completely different behavior. The influence of temperature on the TH curves is not monotonous in the whole applied field, see the crossing of the curves at  $\sim 0.3 \text{ T}$  in Fig. 3(b). Moreover, the TH increases up to the largest fields applied at temperatures below room temperature. The decrease of the TH curves at high enough fields and temperatures can be interpreted as due to a weakening of the pinning strength of the pinned entities, vortices and/or fluxons. The high fields increase of the TH is not compatible with any known magnetic order in carbon-based ferromagnetic

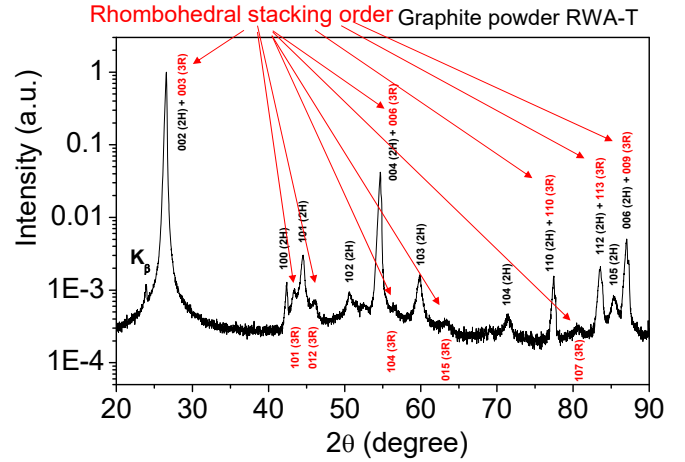


FIG. 4. X-rays diffraction pattern of an ultra pure graphite powder (RWA-T) at room temperature. The labels near the Bragg peaks indicate whether the maximum belong to Bernal (2H) or rhombohedral (3R, in red color) phase. Some of the maxima coincide with both phases within experimental resolution. Adapted from [19].

materials or other typical ferromagnets like magnetite ( $\text{Fe}_3\text{O}_4$ ). On the other hand, similar behavior is measured for granular Y123 high temperature superconductor (unpublished). See also the studies in  $\text{La}_{2-x}\text{Sr}_x\text{CuO}_4$  [15, 16]. The crossing of the TH curves at different temperatures at intermediate applied magnetic fields is related to the granular nature of the superconductivity in the sample.

Finally, magnetization measurements done on bulk highly oriented pyrolytic graphite samples of high grade with interfaces, see Section III, show similar behavior as for the water-treated graphite powder, in contrast to a bulk HOPG sample without or less density of interfaces [8]. Several others experimental studies partially reviewed in [17, 18] indicate that superconductivity is embedded in certain interfaces of the graphite structure. Structural evidence for the existence of interfaces is presented in the next section.

### III. DIRECT EVIDENCE FOR THE EXISTENCE OF INTERFACES IN GRAPHITE

Several electrical resistance measurements of graphite samples of different thickness published in the last years suggest that graphite samples are not homogeneous and that the temperature as well as the absolute value of the electrical resistivity and Hall effect are not unique but thickness- [18, 20–22] and sample-length dependent [23, 24]. Whereas the last dependence is due to the increasing contribution of ballistic transport to the total resistance the smaller the sample length, the thickness dependence observed in the transport properties is mainly



due to the existence of interfaces between the two stacking orders, hexagonal or Bernal (2H) and rhombohedral (3R), see Fig. 4, and between two twinned regions around a common  $c$ -axis, see Fig. 5, with the same or different stacking orders.

Figure 5 shows transmission electron microscope pictures of regions in highly oriented pyrolytic graphite (HOPG) samples (a-c) and of a natural graphite sample (d-f) obtained with the electron beam parallel to the graphene layers. The different gray colors mean a different electron diffraction due to a rotation of the corresponding region respect to a common  $c$ -axis (always normal to the graphene layers) or due to a different stacking order. The 2D interfaces between those regions are very well defined in well ordered samples (a,b,d,e) and less defined or shorter in less ordered graphite samples (e.g. HOPG with grade B, see Fig. 5(c)). The difficulty to pick up from a macroscopic sample a region with a given density of interfaces is clearly demonstrated in the pictures (d-f) where the density of interfaces is not homogeneous in the same natural graphite sample. All these pictures demonstrate the existence of interfaces and the non-homogeneous nature of most of the graphite samples published in the literature [18].

From Fig. 5 it is clear that using graphite samples with thickness smaller than the distance between interfaces, the larger is the probability to measure an intrinsic property of graphite without a large contribution from the interfaces, as has been shown in several recent publications [18, 20–22]. From all those experimental studies we conclude that there are interfaces with metalliclike properties. The metalliclike behavior of the transport properties of graphite is not intrinsic of the graphite ideal structure [18]. Moreover, different theoretical works suggest that some of the interfaces can have superconducting properties as, e.g., between the 2H and 3R stacking orders [26–28] as well as at the interfaces between twinned regions with similar or different stacking orders [25]. According to those theoretical studies, the main reason for the high temperature superconductivity is related to possible flat bands [29–32] that can exist at certain interfaces [33–35] of the graphite structure.

#### IV. CONTACTING THE INTERFACE EDGES IN TEM LAMELLAE

Although signs of granular superconductivity in the electrical resistance of graphite samples with electrodes on the main surface (usually on the top graphene layer) have been recognized in earlier studies [39, 40], if we could contact directly the edges of the interfaces found in graphite samples we expect to observe more clear signs of Josephson or granular superconducting behavior in the transport measurements. As it became evident from the results shown in Fig. 5, added to the unknown position of the possible interfaces with superconducting regions in a given graphite bulk sample, this kind of experimen-

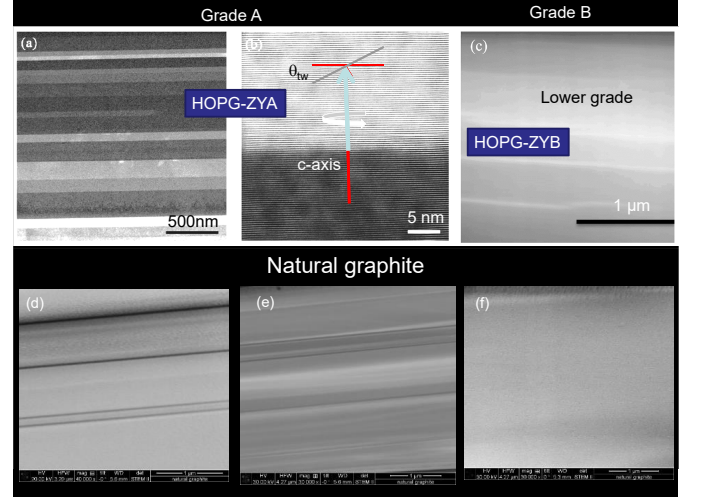


FIG. 5. (a-c): Transmission electron microscope pictures of lamellae taken at low (a) and high resolution (b) on highly oriented pyrolytic graphite (HOPG) samples of grade A and at low resolution on HOPG grade B (c). The pictures were obtained with the electron beam parallel to the graphene layers. The sketch in (b) indicates a possible rotation around the common  $c$ -axis of the two crystalline regions identified through the two different gray colors. (c): The interfaces in this HOPG sample of lower grade are not so well defined as in grade A (a-b) due to the disorder. (d-f): Transmission electron microscope pictures on lamellae from the same natural graphite sample but at different positions. The scale bar at the bottom right indicates  $1 \mu\text{m}$ . Adapted from [17, 19, 20, 25].

tal work is highly time consuming, and was done based mainly on a trial and error strategy. Note that one prepares a TEM lamella of a few micrometers area parallel to the  $c$ -axis, see Fig. 6(a), from a graphite sample of  $\text{mm}^2$  area. Additionally, good electrical contacts on the edges of the interfaces are difficult to prepare after cutting the graphite sample using FIB and  $\text{Ga}^+$  ions.

Several results of different TEM lamellae were published in [37, 38, 41]. Selected results are included in Fig. 6(b-d). The main messages from these results can be summarized as follows: - The voltage of the TEM samples measured at low input currents show a clear drop below a sample dependent temperature, see Fig. 6(b). - The voltage or resistance curves vs. temperature depend strongly on the input current, see Fig. 6(c,d). - The more disordered the graphite structure or the smaller the size or length of the interfaces the lower is the temperature where superconducting-like behavior is observed [41, 42]. - Finally, the  $I-V$  curves measured at different temperatures [37] are compatible with the behavior expected for Josephson junctions under the influence of thermal activation [43]. This means that linear  $I-V$  curves are expected for Josephson junctions at high enough temperatures, as has been measured in high-temperature

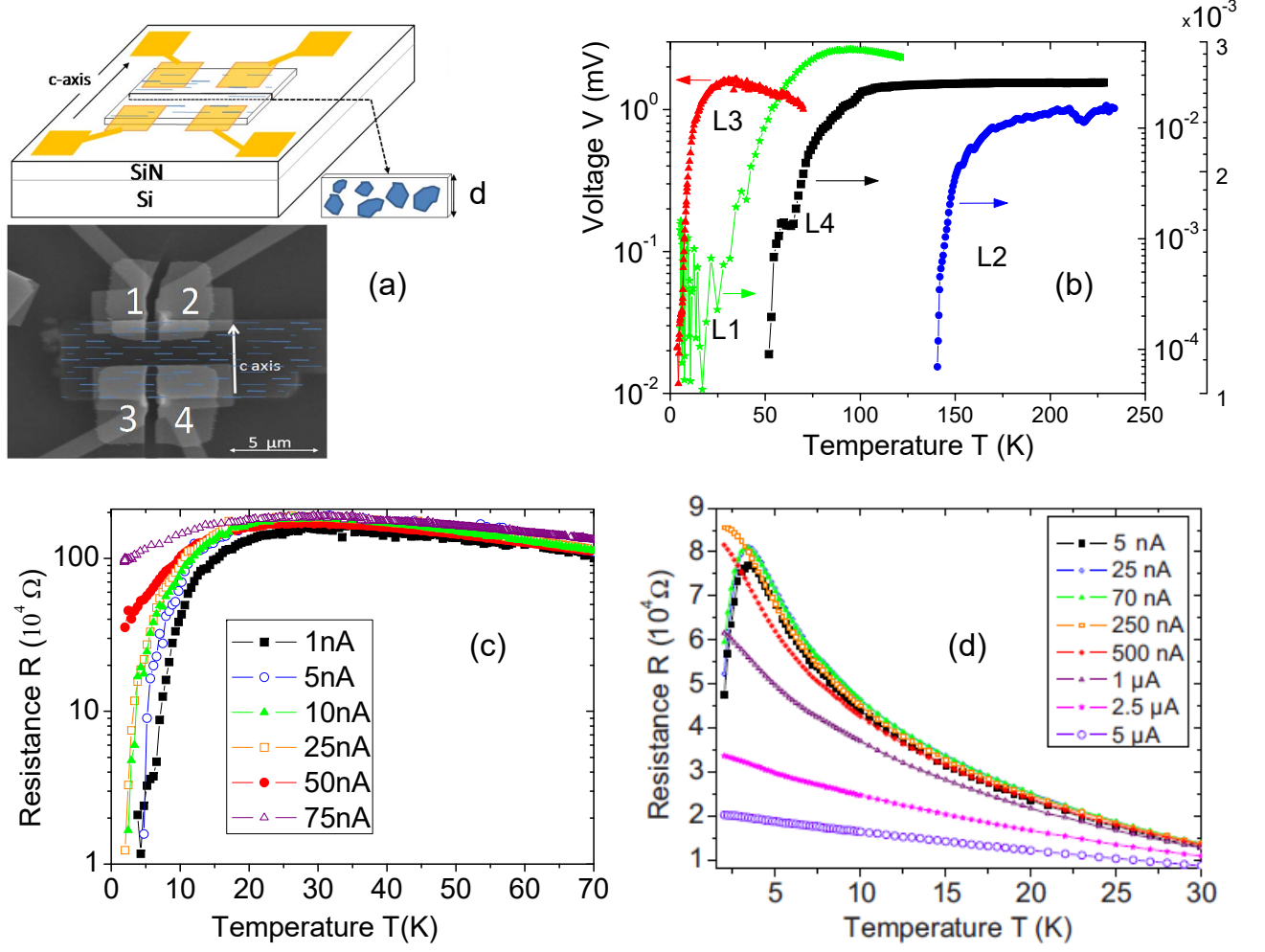


FIG. 6. (a): Sketch of a lamella on a dielectric substrate with four contacts in a Van der Pauw-like configuration. The thickness  $d$  of the lamella can be between 100 nm and 800 nm. Note that the direction of the  $c$ -axis of the graphite structure is parallel to the substrate. The blue short lines indicate the interfaces with probable superconducting regions, i.e. the blue regions in the sketch at the right. Below the sketch we show a SEM picture of a lamella cut from a bulk HOPG sample of grade A [36]. (b) Voltage vs. temperature measured at low input currents from four different lamellae taken from the same HOPG sample of grade A. The second  $y$ -axis corresponds to the lamella L4, adapted from [37]. (c) The resistance vs. temperature for the lamella L3 at different input currents, adapted from [37]. (d) As (c) but for a lamella obtained from a HOPG sample of grade B, see Fig. 5(c), adapted from [38]. All measurements in this figure were done at zero applied field.

superconductors at high enough temperatures [44]. In other words, one could have a sample where due to the size of the superconducting regions and their Josephson coupling the resistance at high temperatures remains finite and nearly ohmic, making difficult to recognize from these measurements alone the existence of superconductivity.

The transport results obtained from TEM lamellae indicate the influence of the Josephson effect on the transport properties, an influence that increases the lower the temperature, where the Josephson coupling and/or the size of the superconducting regions are large enough. The clear decrease in the resistance or voltage at constant current depicted in Fig. 6(b) can be interpreted as due to an

enhancement of the superconducting links between the superconducting regions existing at certain interfaces. In other words, those clear drops in the voltage do not indicate necessarily the critical temperature of those regions. The results discussed in the next section provide a clear evidence for a critical temperature of the superconducting regions above room temperature.

## V. IDENTIFYING THE SUPERCONDUCTING CRITICAL TEMPERATURE

Following the arguments developed in the last section, if the results of magnetization obtained at 300 K, see

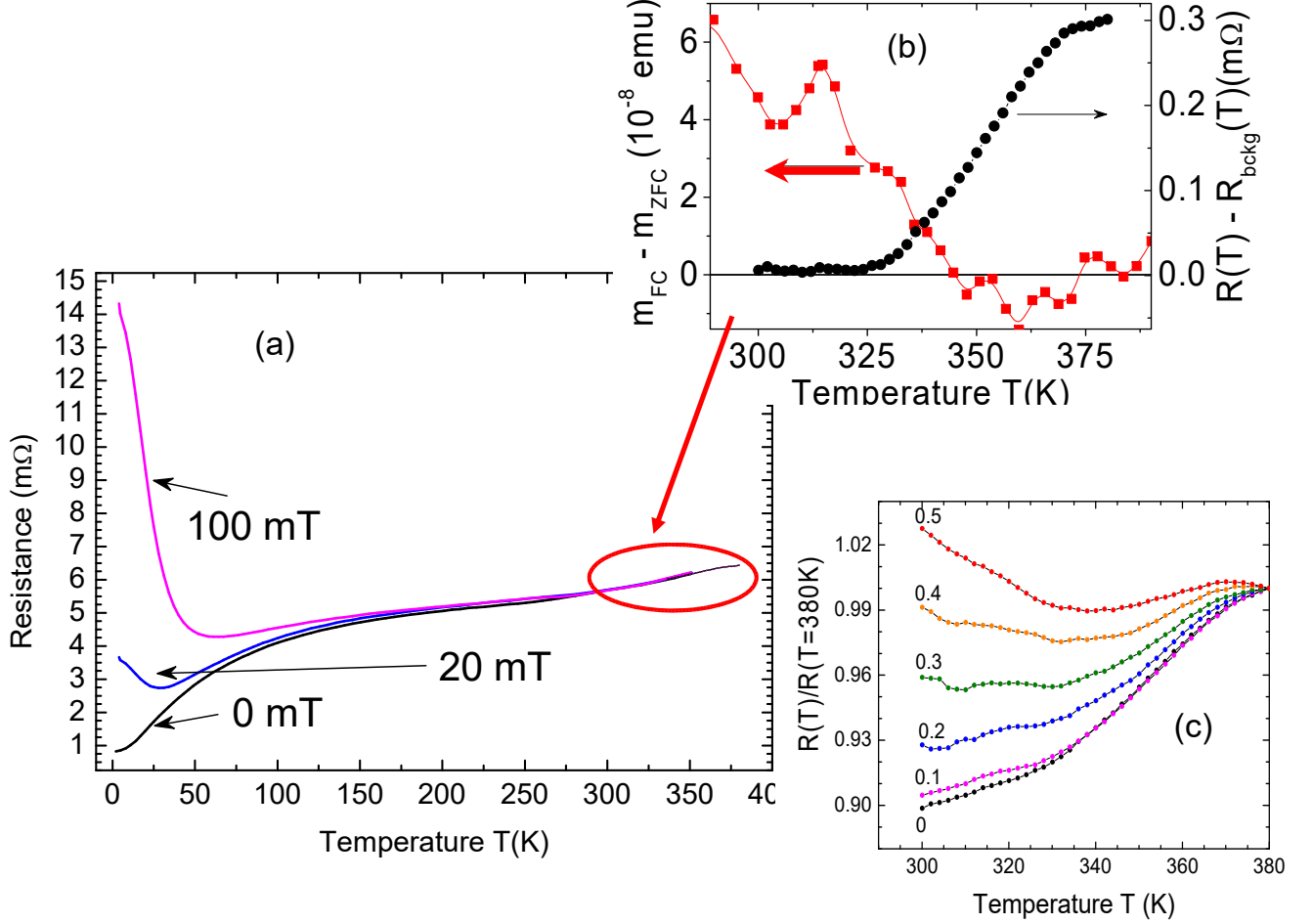


FIG. 7. Temperature dependence of the longitudinal electrical resistance of a natural graphite sample from Brazil. (a): At different magnetic fields applied normal to the graphene planes and interfaces. (b): Temperature dependence of the difference between FC and ZFC magnetic moment (left  $y$ -axis) measured with a SQUID, after applying a field of 50 mT at 250 K with the sample in the virgin state. Right  $y$ -axis: Temperature dependence of the resistance at zero field from (c), after subtracting a straight line background to show the clear change in slope of the measured resistance, indicating a well-defined transition region. (c): Normalized resistance data at high temperatures. The numbers at the curves indicate the field (in Tesla) applied at 380 K and the measurements were done decreasing temperature. The natural graphite sample had 0.4 mm length between voltage electrodes and  $\simeq 1$  mm width. Adapted from [19].

Fig. 2(b) and [8], as well as the results of Fig. 1, are an indication of superconductivity, we then should expect a critical temperature clearly above room temperature. To identify it, high-resolution electrical resistance measurements on different natural graphite samples as well as HOPG samples were reported recently [19]. The main results obtained in a natural graphite sample from a Brazil mine are shown in Figs. 7 and 8. The resistance of the sample was measured with four electrodes at the top surface. The temperature dependence of the resistance for three different magnetic fields applied normal to the graphene and interface planes is shown in Fig. 7(a). The huge magnetic field driven metal-insulator transition (MIT) at  $T < 150$  K is especially large for the measured natural graphite sample. This field driven MIT

in graphite was speculated in the past to be related to superconductivity [45, 46]. Nowadays we know that the MIT in graphite as well as the metalliclike behavior of its resistance are not intrinsic but are due to the contribution of certain interfaces in parallel to the graphene layers of the graphite structure [18, 20, 21].

If one measures the resistance with care, see [19] for more details, one can identify an anomaly at  $T \sim 350$  K for that sample. After subtracting a linear in temperature background to the measured resistance we obtain the curve in Fig. 7(b), which clearly shows a transition-like behavior. The TH at a field of 50 mT is shown in the same figure, which result indicates the start of an irreversibility at a similar temperature as the transition in the resistance. Figure 7(c) shows the temperature de-

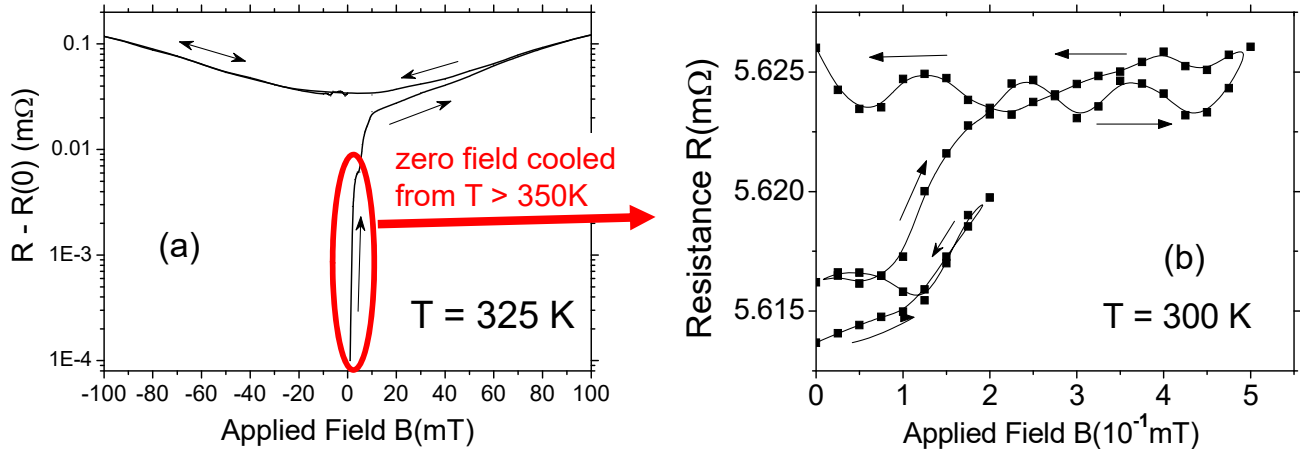


FIG. 8. (a) Difference between the resistance and its value at zero field vs. applied field in two opposite directions at 325 K measured in a natural graphite sample. The arrows indicate the sweep field direction. The virgin state is reached after zero field cooling the sample from temperature above 350 K. (b) Similar as in (a) but at 300 K and at very low fields starting from the virgin state after ZFC from 390 K. Note the clear remanence after decreasing the magnetic field to zero. Adapted from [19].

pendence of the normalized resistance at different applied fields. The magnetoresistance results also indicate the existence of an anomaly at such high temperatures.

A support for the interpretation of a superconducting transition at such high temperatures is given by the large irreversibility and remanence measured in the resistance [19]. As an example, we show in Fig. 8 the irreversibility in the magnetoresistance at  $T < T_c$  after ZFC from  $T > 350$  K. The fact that no magnetoresistance is measurable in this field range or higher within a relative resolution better than  $10^{-5}$  when the field is applied parallel to the interfaces, rules out a relation of the transition to a magnetic order phenomenon.

Because the superconducting regions are thought to be within certain interfaces, there is no simple experimental method to demonstrate zero electrical resistance below  $T_c$ , unless one tries to contact directly the superconducting regions, which location within the sample and within a given interface remains unknown. Moreover, if the size of the superconducting regions is much smaller than the effective London penetration depth, in addition to demagnetization effects, the flux expulsion, i.e. the Meissner effect, would be practically immeasurable. An alternative proof for the existence of superconductivity, i.e. of a region in the sample with real zero resistance, can rely on the observation of dissipationless currents that maintain a magnetic flux trapped at certain regions of the sample. Using magnetic force microscopy (MFM) we were able to localize a permanent current path that was triggered in a natural graphite bulk sample after removing an applied magnetic field, i.e. at remanence [47], as expected from the results shown in Fig. 8.

Figure 9(a) shows the line scans of the phase measured with a MFM tip and obtained across the current line re-

gion, see Fig. 9(k), measured at 293 K. The measured curve is compatible with the existence of a electrical current path, as the measurements on a Au current loop, Figs 9(h-i) and the theoretical line scan in Fig. 9(j) indicate. The amplitude of the jump in the line scan  $\Delta\varphi$ , defined in Fig. 9(a), is proportional to the current amplitude. The temperature dependence of this phase jump shown in Fig. 9(l) vanishes irreversibly at the same transition temperature obtained by the electrical resistance and the remanence for the same sample, for more details see [47].

## VI. CONCLUSION

The experimental facts obtained the last years provide evidence for 2D granular superconductivity at certain interfaces in graphite. High resolution transport and magnetization measurements, as well as MFM indicate the existence of a transition at a critical temperature  $T_c \gtrsim 350$  K. The remanence in the electrical resistance as well as the phase signals obtained from MFM provide evidence for persistent currents up to  $T_c$ , evidence that indicate the existence of regions with negligible electrical resistance. On the other hand there is a “critical temperature”  $T_c^J$ , below which the Josephson coupling between grains is large enough to strongly influence the electrical resistance of graphite samples with interfaces. This  $T_c^J$  depends on the interface size and/or internal order in the graphite structure. There are several open questions to be answered in the future. Namely how large are the critical fields, are protons (or hydrogen) playing any role at the interfaces, and how to produce specific interfaces? A real help for experimentalists is the possibility



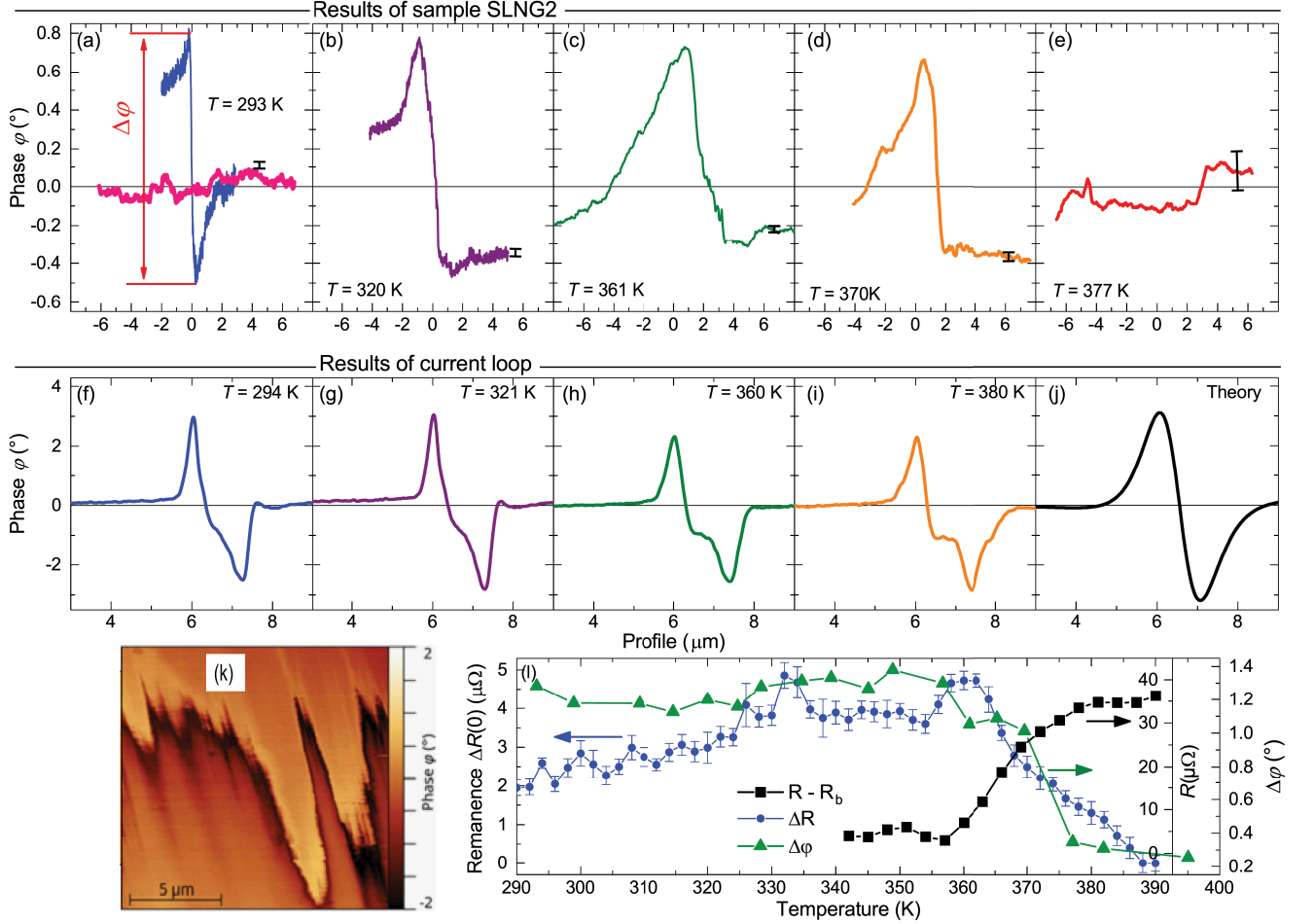


FIG. 9. (a)–(e): Line scans of the field gradient at different temperatures obtained at the edges of the trapped flux region in remanence. The error bars represent the standard deviation of the phase at the given temperature. The blue curve in (a) is the measured line scan with the sample in remanent state and the purple color curve is the line scan at the same position but cooling the sample at zero field after reaching 395 K and the magnetic flux vanishes, see (l). (f–i): The same but for a current loop of Au of ring geometry and with  $\approx 1 \mu\text{m}$  width prepared by electron lithography. A theoretical phase shift is shown in (j), obtained from a simulated current line loop of ring geometry and zero width. The phase image (k) shows a small part of the whole current loop in a region of the sample surface where the current path is measured (the dark edge between the regions of different phase colors). The meandering structure of the current path shown by the MFM phase line looks similar to the one observed in high-temperature superconducting oxides in remanence [48, 49]. The line scans of the phase (a–e) were taken normal to the current line. In Fig.(l), the phase difference  $\Delta\varphi$  (see (a)), the resistance  $R$  (after a linear background subtraction) and the remanence  $\Delta R(0)$  (see [19] for details on the remanence measurements) are shown as function of temperature. Adapted from [47].

to use scanning magnetic imaging techniques to identify the regions of graphite samples where superconductivity is localized. This will undoubtedly help to answer some of the open questions and further characterize the superconducting regions in graphite. If the production of specific graphite interfaces turns out to be very difficult, the localization of the superconducting regions would already pave the way for future device implementations of graphite mine flakes, which costs nowadays are much less than an artificial production.

## ACKNOWLEDGMENTS

We thank Ana Champi and Henning Beth for discussions and support and for providing us with the natural graphite samples. We thank T. Heikkilä, G. Volovik, and J. Meijer for fruitful discussions. C.E.P. gratefully acknowledges the support provided by The Brazilian National Council for the Improvement of Higher Education (CAPES). M.S. and J.B-Q. are supported by the DFG collaboration project SFB762.

- 
- [1] K. Antonowicz, *Nature* **247**, 358 (1974)
- [2] K. Antonowicz, *phys. stat. sol. (a)* **28**, 497 (1975)
- [3] M. Tinkham, *Introduction to Superconductivity* (McGraw Hill International Editions, 1996)
- [4] H.B. Heersche, P. Jarillo-Herrero, J.B. Oostinga, L.M.K. Vandersypen, A.F. Morpurgo, *Nature* **446**, 56 (2007)
- [5] J. Pearl, *Applied Physics Letters* **5**, 65 (1964)
- [6] S. Shapiro, *Phys. Rev. Lett.* **11**, 80 (1963)
- [7] T. Scheike, W. Böhlmann, P. Esquinazi, J. Barzola-Quiquia, A. Ballestar, A. Setzer, *Adv. Mater.* **24**, 5826 (2012)
- [8] T. Scheike, P. Esquinazi, A. Setzer, W. Böhlmann, *Carbon* **59**, 140 (2013)
- [9] B. Andrzejewski, E. Guilmeau, C. Simon, *Supercond. Sci. Technol.* **14**, 904 (2001)
- [10] S. Senoussi, C. Aguilon, S. Hadjoudj, *Physica C* **175**, 215 (1991)
- [11] Y. Kawashima, *AIP Advances* **3**, 052132 (2013)
- [12] Y. Kopelevich, P. Esquinazi, J. Torres, S. Moehlecke, *J. Low Temp. Phys.* **119**, 691 (2000)
- [13] D. Spemann, P. Esquinazi, A. Setzer, W. Böhlmann, *AIP Advances* **4**, 107142 (2014)
- [14] H. Ohldag, P. Esquinazi, E. Arenholz, D. Spemann, M. Rothermel, A. Setzer, T. Butz, *New Journal of Physics* **12**, 123012 (2010)
- [15] C. Panagopoulos, M. Majoros, A.P. Petrović, *Phys. Rev. B* **69**, 144508 (2004)
- [16] M. Majoros, C. Panagopoulos, T. Nishizaki, H. Iwasaki, *Phys. Rev. B* **72**, 024528 (2005)
- [17] P. Esquinazi, *Papers in Physics* **5**, 050007 (2013)
- [18] P. Esquinazi, Y. Lysogorskiy, *Experimental evidence for the existence of interfaces in graphite and their relation to the observed metallic and superconducting behavior* (P. Esquinazi (ed.), Springer International Publishing AG Switzerland, 2016), pp. 145–179. Springer Series in Materials Science 244
- [19] C.E. Precker, P.D. Esquinazi, A. Champi, J. Barzola-Quiquia, M. Zoraghi, S. Muñios-Landin, A. Setzer, W. Böhlmann, D. Spemann, J. Meijer, T. Muenster, O. Baehre, G. Kloess, H. Beth, *New J. Phys.* **18**, 113041 (2016)
- [20] J. Barzola-Quiquia, J.L. Yao, P. Rödiger, K. Schindler, P. Esquinazi, *phys. stat. sol. (a)* **205**, 2924 (2008)
- [21] M. Zoraghi, J. Barzola-Quiquia, M. Stiller, A. Setzer, P. Esquinazi, G.H. Kloess, T. Muenster, T. Löhmann, I. Estrela-Lopis, *Phys. Rev. B* **95**, 045308 (2017)
- [22] P. Esquinazi, J. Krüger, J. Barzola-Quiquia, R. Schönemann, T. Hermannsdörfer, N. García, *AIP Advances* **4**, 117121 (2014)
- [23] S. Dusari, J. Barzola-Quiquia, P. Esquinazi, N. García, *Phys. Rev. B* **83**, 125402 (2011)
- [24] P. Esquinazi, J. Barzola-Quiquia, S. Dusari, N. García, *J. Appl. Phys.* **111**, 033709 (2012)
- [25] P. Esquinazi, T.T. Heikkilä, Y.V. Lysogorskiy, D.A. Tayurskii, G.E. Volovik, *JETP Letters* **100**, 336 (2014). arXiv:1407.1060
- [26] W.A. Muñoz, L. Covaci, F. Peeters, *Phys. Rev. B* **87**, 134509 (2013)
- [27] N.B. Kopnin, M. Ijäs, A. Harju, T.T. Heikkilä, *Phys. Rev. B* **87**, 140503 (2013)
- [28] N.B. Kopnin, T.T. Heikkilä, *Carbon-based Superconductors: Towards High- $T_c$  Superconductivity* (Pan Stanford Publishing, CRC Press, Taylor & Francis Group, 2015), chap. 9, pp. 231–263. arXiv:1210.7075
- [29] N.B. Kopnin, T.T. Heikkilä, G.E. Volovik, *Phys. Rev. B* **83**, 220503 (2011)
- [30] G.E. Volovik, *J Supercond Nov Magn* **26**, 2887 (2013)
- [31] T. Heikkilä, G.E. Volovik, *Flat bands as a route to high-temperature superconductivity in graphite* (P. Esquinazi (ed.), Springer International Publishing AG Switzerland, 2016), pp. 123–144. Springer Series in Materials Science 244
- [32] V.J. Kauppila, F. Aikebaier, T.T. Heikkilä, *Phys. Rev. B* **93**, 214505 (2016)
- [33] L. Feng, X. Lin, L. Meng, J.C. Nie, J. Ni, L. He, *Appl. Phys. Lett.* **101**, 113113 (2012)
- [34] C. Coletti, S. Forti, A. Principi, K.V. Emtsev, A.A. Zakharov, K.M. Daniels, B.K. Daas, M.V.S. Chandrashekhara, T. Ouisse, D. Chaussende, A.H. MacDonald, M. Polini, U. Starke, *Phys. Rev. B* **88**, 155439 (2013)
- [35] D. Pierucci, H. Sediri, M. Hajlaoui, J.C. Girard, T. Brumme, M. Calandra, E. Velez-Fort, G. Patriarche, M.G. Silly, G. Ferro, V. Souliere, M. Marangolo, F. Sirotti, F. Mauri, A. Ouerghi, *ACS Nano* **9**, 5432 (2015)
- [36] Ana Ballestar, Ph.D. Thesis entitled "Superconductivity at Graphite interfaces", University of Leipzig (2014), unpublished
- [37] A. Ballestar, J. Barzola-Quiquia, T. Scheike, P. Esquinazi, *New J. Phys.* **15**, 023024 (2013)
- [38] A. Ballestar, P. Esquinazi, W. Böhlmann, *Phys. Rev. B* **91**, 014502 (2015)
- [39] P. Esquinazi, N. García, J. Barzola-Quiquia, P. Rödiger, K. Schindler, J.L. Yao, M. Ziese, *Phys. Rev. B* **78**, 134516 (2008)
- [40] S. Dusari, J. Barzola-Quiquia, P. Esquinazi, *J Supercond Nov Magn* **24**, 401 (2011)
- [41] A. Ballestar, T.T. Heikkilä, P. Esquinazi, *Superc. Sci. Technol.* **27**, 115014 (2014)
- [42] J. Barzola-Quiquia, P. Esquinazi, M. Lindel, D. Spemann, M. Muallem, G. Nessim, *Carbon* **88**, 16 (2015)
- [43] V. Ambegaokar, B.I. Halperin, *Phys. Rev. Lett.* **22**, 1364 (1969)
- [44] R. Gross, P. Chaudhari, D. Dimos, A. Gupta, G. Koren, *Phys. Rev. Lett.* **64**, 228 (1990)
- [45] H. Kempa, Y. Kopelevich, F. Mrowka, A. Setzer, J.H.S. Torres, R. Höhne, P. Esquinazi, *Solid State Commun.* **115**, 539 (2000)
- [46] Y. Kopelevich, P. Esquinazi, J.H.S. Torres, R.R. da Silva, H. Kempa, *Graphite as a highly correlated electron liquid* (B. Kramer (Ed.), Springer-Verlag Berlin, 2003), *Advances in Solid State Physics*, vol. 43, pp. 207–222
- [47] C.E.P. M. Stiller, P. D. Esquinazi, J. Barzola-Quiquia, Local magnetic measurements of permanent current paths in a natural graphite crystal. arXiv:1705.09909
- [48] V.K. Vlasko-Vlasov, U. Welp, G.W. Crabtree, D. Gunter, V. Kabanov, V.I. Nikitenko, *Phys. Rev. B* **56**, 5622 (1997)
- [49] V.K. Vlasko-Vlasov, U. Welp, C.G. W., D. Gunter, V. Kabanov, V.I. Nikitenko, L.M. Paulius, *Phys. Rev. B* **58**, 3446 (1998)